

Current Biology

Rhizosphere-Associated *Pseudomonas* Suppress Local Root Immune Responses by Gluconic Acid-Mediated Lowering of Environmental pH

Highlights

- 42% of the tested root microbiota are able to quench local root immune responses
- Beneficial *Pseudomonas* can suppress root immunity by lowering environmental pH
- Suppression of immunity facilitates root colonization by these beneficial microbes

Authors

Ke Yu, Yang Liu, Ramon Tichelaar, ..., Peter A.H.M. Bakker, Cara H. Haney, Roeland L. Berendsen

Correspondence

r.l.berendsen@uu.nl

In Brief

Many plant-root-associated microbes can trigger plant defenses. Yu et al. show that the production of gluconic acid and its derivative 2-keto gluconic acid acidifies the plant growth medium, suppressing flg22-induced root immunity to facilitate colonization by beneficial root microbiota.



Rhizosphere-Associated *Pseudomonas* Suppress Local Root Immune Responses by Gluconic Acid-Mediated Lowering of Environmental pH

Ke Yu,¹ Yang Liu,² Ramon Tichelaar,¹ Niharika Savant,¹ Ellen Legendijk,³ Sanne J.L. van Kuijk,¹ Ioannis A. Stringlis,¹ Anja J.H. van Dijken,¹ Corné M.J. Pieterse,¹ Peter A.H.M. Bakker,¹ Cara H. Haney,² and Roeland L. Berendsen^{1,4,*}

¹Plant-Microbe Interactions, Institute of Environmental Biology, Department of Biology, Science4Life, Utrecht University, 3508 CH Utrecht, the Netherlands

²Department of Microbiology & Immunology, University of British Columbia, Vancouver, BC V6T 1Z4, Canada

³Koppert Biological Systems B.V., R&D Microbiology – Process Development, Veilingweg 14, 2651 BE Berkel en Rodenrijs, the Netherlands

⁴Lead Contact

*Correspondence: r.l.berendsen@uu.nl

<https://doi.org/10.1016/j.cub.2019.09.015>

SUMMARY

The root microbiome consists of commensal, pathogenic, and plant-beneficial microbes [1]. Most members of the root microbiome possess microbe-associated molecular patterns (MAMPs) similar to those of plant pathogens [2]. Their recognition can lead to the activation of host immunity and suppression of plant growth due to growth-defense tradeoffs [3, 4]. We found that 42% of the tested root microbiota, including the plant growth-promoting rhizobacteria *Pseudomonas capeferrum* WCS358 [5, 6] and *Pseudomonas simiae* WCS417 [6, 7], are able to quench local *Arabidopsis thaliana* root immune responses that are triggered by flg22 [8], an immunogenic epitope of the MAMP flagellin [9], suggesting that this is an important function of the root microbiome. In a screen for WCS358 mutants that lost their capacity to suppress flg22-induced *CYP71A12_{pro}:GUS* MAMP-reporter gene expression, we identified the bacterial genes *pqqF* and *cyoB* in WCS358, which are required for the production of gluconic acid and its derivative 2-keto gluconic acid. Both WCS358 mutants are impaired in the production of these organic acids and consequently lowered their extracellular pH to a lesser extent than wild-type WCS358. Acidification of the plant growth medium similarly suppressed flg22-induced *CYP71A12_{pro}:GUS* and *MYB51_{pro}:GUS* expression, and the flg22-mediated oxidative burst, suggesting a role for rhizobacterial gluconic acid-mediated modulation of the extracellular pH in the suppression of root immunity. Rhizosphere population densities of the mutants were significantly reduced compared to wild-type. Collectively, these findings show that suppression of immune responses is an important function of the root

microbiome, as it facilitates colonization by beneficial root microbiota.

RESULTS

The Plant-Beneficial Rhizobacteria WCS417 and WCS358 Both Suppress Root Immune Responses

To uncover mechanisms by which beneficial rhizobacteria interfere with the plant immune system that limits their proliferation [10], we investigated the suppression of flg22-triggered root immune responses by rhizosphere inhabitants. We employed three *Arabidopsis* transgenic lines carrying β -glucuronidase (GUS) reporters *CYP71A12_{pro}:GUS*, *MYB51_{pro}:GUS*, and *WRKY11_{pro}:GUS*. All three reporter lines display high GUS activity in the root elongation zone when treated with the flg22 epitope (Figures 1A and S1A; [8, 11]). To test the effect of plant-beneficial rhizobacteria on flg22-induced root responses, we pre-inoculated roots of *Arabidopsis* seedlings with WCS417 or WCS358, 18 h prior to treatment with flg22. We found that live WCS417 and WCS358 cells, which produce immune-eliciting flagellin, did not induce GUS expression in the root elongation zone (Figures 1A and S1A). Moreover, both WCS417 and WCS358 suppressed flg22-induced GUS expression in the root elongation zone (Figures 1A and S1A), supporting previous findings [8]. The rhizobacteria-mediated suppression of *CYP71A12_{pro}:GUS* is not dependent on synthesis or signaling of the hormones salicylic acid (SA) and jasmonic acid (JA) (Figure S2A). Furthermore, filter sterilized root exudates in which WCS417 and WCS358 had grown similarly suppressed flg22-induced *CYP71A12_{pro}:GUS* (Figure 1A), indicating that bacteria secrete the immune-suppressive compound. Moreover, heat treatment of these filtrates did not affect the ability to suppress flg22-induced *CYP71A12_{pro}:GUS* (Figure 1A), suggesting that the immune-suppressive compounds produced by WCS417 and WCS358 are not proteinaceous.

Only a small subset of *Arabidopsis*-associated bacterial species possesses genes that encode the flg22 epitope [12], and examples of plant-beneficial bacteria that have evolved divergent flagellin molecules to evade host immune recognition have been described [13, 14]. Although the flg22 epitopes derived from WCS417 (flg22⁴¹⁷) and WCS358 (flg22³⁵⁸) are distinct



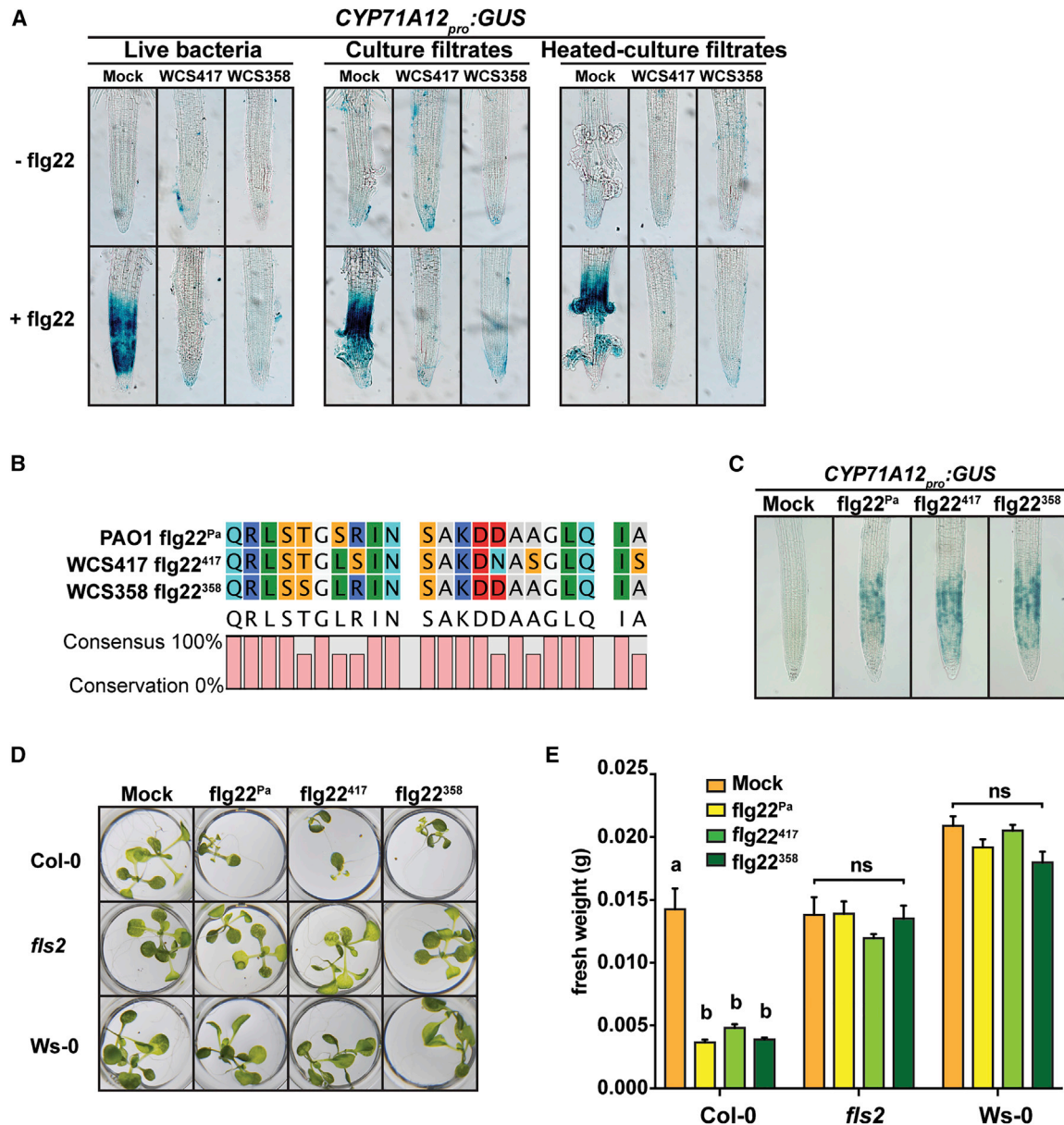


Figure 1. Flg22 Epitopes Derived from *Pseudomonas* spp. Strains WCS417 and WCS358 Induce Defense Responses in *Arabidopsis thaliana*
 (A) Effects of live cells, culture filtrates, and heat-treated culture filtrates of WCS417 and WCS358 on flg22-induced *CYP71A12_{pro}:GUS* expression in the root elongation zone.
 (B) Sequence alignment of flg22 epitopes derived from *P. aeruginosa* PAO1 (flg22^{Pa}), *P. simiae* WCS417 (flg22⁴¹⁷), and *P. capeferrum* WCS358 (flg22³⁵⁸).
 (C) Effects of flg22^{Pa}, flg22⁴¹⁷, and flg22³⁵⁸ on *CYP71A12_{pro}:GUS* expression in the root elongation zone of *Arabidopsis* seedlings.
 (D) Effects of flg22^{Pa}, flg22⁴¹⁷, and flg22³⁵⁸ peptides on growth of Col-0, *fls2*, and *Ws-0* seedlings.
 (E) Fresh weight of *Arabidopsis* seedlings shown in (D). The bars depict the average of five replicates. Error bars represent SEM. Letters indicate significant differences (one-way ANOVA followed by Tukey's test; $p < 0.05$; ns, not significant). [Figure S1](#) shows the effect on *MYB51_{pro}:GUS* *WRKY11_{pro}:GUS* expression. See also [Figures S1](#) and [S2](#) and [STAR Methods](#).

from each other as well as from the standard *Pseudomonas aeruginosa* PAO1 flg22 (flg22^{Pa}; [Figure 1B](#)), they all triggered flg22-induced defense responses in the root elongation zone ([Figures 1C](#) and [S1B](#)) and inhibited growth of Col-0 seedlings through growth-defense tradeoffs in a flagellin receptor FLS2-dependent manner ([Figures 1D](#) and [1E](#)), confirming previous findings [[4](#), [8](#), [15](#), [16](#)].

Diverse Rhizobacteria Suppress flg22-Induced Immune Responses in *Arabidopsis* Roots

To investigate whether the ability to suppress root immune responses is a general phenomenon among different members of the root microbiome, we screened 28 taxonomically diverse bacterial strains isolated from the *Arabidopsis* rhizosphere [[17](#)] for their effects on *CYP71A12_{pro}:GUS* expression in the root

elongation zone in the presence or absence of flg22. With the exception of five strains, the majority of rhizobacteria did not induce *CYP71A12_{pro}:GUS* in the absence of flg22, suggesting that these bacteria avoid MAMP-triggered immune responses in the roots (Table S1). In the presence of flg22, 10 of the 28 bacterial strains tested suppressed flg22-induced *CYP71A12_{pro}:GUS* in the root elongation zone. Together, these results indicate that the rhizosphere microbiome contains members that are capable of activating MAMP-triggered immune responses in plant roots, but also a large diversity of microbiota members that actively suppress it.

Root Immune Suppression Mediated by WCS358 Requires PqqF and CyoB

To investigate the bacterial determinants of WCS358-mediated root immune suppression, we screened a mini-Tn5 transposon insertion mutant library for mutants that failed to suppress flg22-induced *CYP71A12_{pro}:GUS*. We found 32 mutants that were consistently unable to suppress flg22-induced *CYP71A12_{pro}:GUS*. Thirty of these were severely impaired in growth when cultivated in root exudates, which likely explained their inability to suppress local root immune responses. In the remaining 2 mutants, arbitrary PCR mapped the Tn5 transposon insertion sites to two genes: *pqqF* (PC358_RS24460) and *cyoB* (PC358_RS16700). Both mutants were unable to suppress flg22-induced *CYP71A12_{pro}:GUS* in the root elongation zone (Figure 2A), and their growth in root exudates was significantly increased compared to wild-type WCS358 (Figure 2B). Nonetheless, culture filtrates from both *pqqF::Tn5* and *cyoB::Tn5* failed to suppress this response (Figure 2C), suggesting that the production of the immune-suppressive diffusible compound(s) is impaired in both mutants. Although these mutants did not visibly induce *CYP71A12_{pro}:GUS* without exogenous application of flg22, both mutants induced *CYP71A12* expression in *Arabidopsis* roots to significantly higher levels than wild-type WCS358 (Figure 2D). These results suggest that both PqqF and CyoB are essential in root immune suppression mediated by WCS358.

Root Immune Suppression Mediated by WCS358 Relies on Gluconic Acid Production

PqqF is a putative protease required for pyrroloquinoline quinone (PQQ) biosynthesis [18]. PQQ is a redox active molecule, functioning as a cofactor for many bacterial dehydrogenases involved in the utilization of carbon sources [19]. CyoB is the subunit I of terminal ubiquinol cytochrome *bo*₃ oxidase (CYO) complex, a macromolecular protein embedded in the cytoplasmic membrane [20]. CYO functions in the aerobic respiratory chain for energy generation and regulates the expression of genes involved in the utilization of carbon sources [21]. PQQ and CYO play important roles in bacterial oxidative fermentation of glucose, resulting in production of D-gluconic acid (GA) and 2-keto-D-gluconic (2-KGA) [22]. We analyzed culture filtrates from WCS358, its derivatives *pqqF::Tn5* and *cyoB::Tn5*, and of *P. simiae* WCS417 by using ultra-performance liquid chromatography-mass spectrometry (UPLC-MS) and found that both wild-type bacteria produced both GA and 2-KGA (Figure 2E). Mutation of *pqqF* completely abolished the production of both GA and 2-KGA, whereas mutation of *cyoB* moderately reduced the production of GA and abolished the production of 2-KGA

(Figure 2E). Notably, WCS417 produced a significantly higher amount of GA than wild-type WCS358. Production of these organic acids can substantially decrease extracellular pH [22]. Indeed, the pH of culture filtrates from wild-type WCS358 (pH 3.7) and WCS417 (pH 3.5) growing on root exudates was significantly lower than that of culture filtrates derived from mutant *pqqF::Tn5* or *cyoB::Tn5* (pH 4.2 and 4.3, respectively; Figure 2F), suggesting that WCS358 acidifies its extracellular environment through the production of GA and 2-KGA.

The magnitude of flg22-induced immune responses in *Arabidopsis* changes dramatically when environmental pH varies [23]. We reasoned that WCS358 may suppress root immune responses by acidifying its environment and therefore examined how the pH of the plant growth medium affects flg22-induced *CYP71A12_{pro}:GUS*. When the pH was adjusted to 3.7 by adding either HCl or GA, flg22-induced *CYP71A12_{pro}:GUS* was completely abolished (Figures 2G and 2H). However, at pH 4.6 or higher, *CYP71A12_{pro}:GUS* was still induced by flg22 (Figure 2G). We noticed that the timing of adjusting the pH is crucial. Only when the pH was modified immediately before addition of flg22 did we find the suppressive effect of pH on flg22-induced *CYP71A12_{pro}:GUS* (Figure 2I). When the pH was modified to 3.7 at 18 h before application of flg22, the pH of the growth medium was restored to 5.3 at the moment of flg22 application, and suppression of flg22-induced *CYP71A12_{pro}:GUS* was alleviated (Figure 2I), highlighting that plant roots actively modify their environmental acidity. Acidification of the plant apoplast by the fungal pathogen *Sclerotinia sclerotiorum* can suppress immunity and the local oxidative burst via oxalic acid production; a *S. sclerotiorum* mutant that cannot secrete oxalic acid induces an enhanced oxidative burst in plants [24]. We tested whether acidification by gluconic acid could similarly suppress the flg22-triggered oxidative burst in *Arabidopsis* seedlings. We found that lowering the pH of the media to 3.7 with GA or HCl resulted in a complete suppression of the flg22-triggered oxidative burst (Figure 2J), indicating that acidification suppresses multiple downstream flg22-dependent immune responses.

Gluconic Acid Is a Conserved Means to Suppress Plant Immunity across Diverse *Pseudomonas* spp

To test whether PQQ biosynthesis is required for suppression of *CYP71A12_{pro}:GUS* in diverse *Pseudomonas* spp. strains, we obtained transposon insertion mutants from an ordered library in the opportunistic pathogenic *P. aeruginosa* strain PAO1 [25]. The *pqqABCDEH*, *pqqF*, and *cyoABCDE* genes are conserved between PAO1 and WCS358 and most other *Pseudomonas* spp. (Figure S3). *P. aeruginosa* strains are found throughout the environment and can have properties ranging from plant-beneficial [26] to pathogenic in plants and animals [27]. We tested insertion mutants in *pqqB* (insertion at position 726 bp) and *pqqD* (position 82 bp), two insertion mutants in *pqqF* (positions 451 and 1447 bp) and two in *pqqH* (positions 529 and 1641 bp), and a mutant with an insertion in *cyoB* (834 bp). We found that unlike wild-type PAO1, transposon mutants of *pqqB*, *pqqD*, *ppqF*, *pqqH*, and *cyoB* were unable to suppress flg22-induced *CYP71A12_{pro}:GUS* (Figure 3A). This suggests that suppression of root immunity by *Pseudomonas* spp. is conserved and relies on the ability to acidify the root environment.

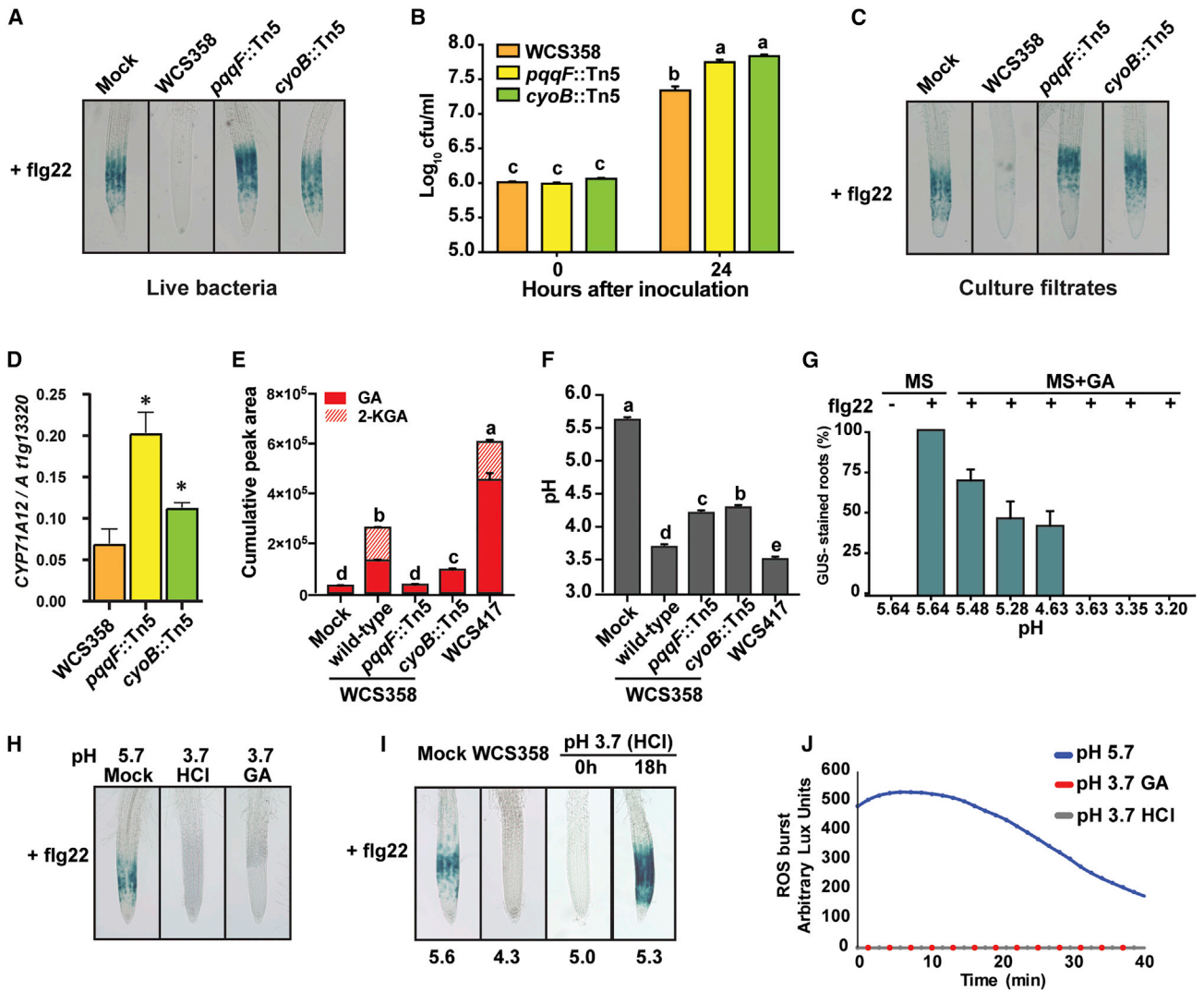


Figure 2. WCS358 Suppresses flg22-Induced Immune Responses in Arabidopsis Roots by Producing GA and 2-KGA

(A) Effects of wild-type WCS358 and its mutant derivatives *pqqF::Tn5* and *cyoB::Tn5* on flg22-induced *CYP71A12_{pro}:GUS* expression in the root elongation zone.

(B) Growth of WCS358 and its derivatives *pqqF::Tn5* and *cyoB::Tn5* in root exudates of *Arabidopsis* seedlings. The y axis shows the log₁₀ of colony-forming units (CFU) per mL of root exudates. The data shown are means of eight replicates. Error bars represent SEM. Letters indicate significant difference (two-way ANOVA followed by Tukey's test; $p < 0.05$).

(C) Effects of sterile culture filtrates derived from wild-type WCS358 and its derivatives *pqqF::Tn5* and *cyoB::Tn5* on flg22-induced *CYP71A12_{pro}:GUS* expression in the root elongation zone.

(D) Gene expression profiles of *CYP71A12* in WCS358-, *pqqF::Tn5*-, and *cyoB::Tn5*-treated *Arabidopsis* Col-0 roots quantified by qRT-PCR. For qRT-PCR, transcript levels were normalized to that of reference gene *PP2AA3* (*At1g13320*). Data are means of three biological replicates. Error bars represent SD. Asterisks represent statistically significant differences with expression level of WCS358-treated roots (Student's *t* test; $p < 0.05$).

(E) HPLC-MS measurement of GA and 2-KGA shown as the cumulative peak area (GA + 2-KGA) of mass spectra detected in 2 channels on a UPLC-MS in negative ionization mode.

(F) Acidity in the culture filtrates derived from wild-type WCS358, its derivatives *pqqF::Tn5* and *cyoB::Tn5*, and WCS417.

The data shown in (E) and (F) are means of three replicates. Error bars represent SEM. Letters indicate significant differences (one-way ANOVA followed by Tukey's test; $p < 0.05$).

(G) Effects of a pH gradient on flg22-induced *CYP71A12_{pro}:GUS* expression in the root elongation zone. Ratio of root tips with *CYP71A12_{pro}:GUS* expression as a percentage of total root tips. The data shown are average percentage of three replicate wells containing 10–15 seedlings. Error bars represent SEM.

(H) Effects of low environmental pH on flg22-induced *CYP71A12_{pro}:GUS* expression in the root elongation zone. HCl and GA were used to adjust the pH of root exudates to 3.7.

(I) Effects of 18 h of pre-incubation in low environmental pH on flg22-induced *CYP71A12_{pro}:GUS* expression in the root elongation zone. The pH shown under each picture was measured immediately before GUS staining.

(J) Acidification suppresses the flg22-triggered ROS burst in *Arabidopsis* seedlings.

See also Figure S2 and STAR Methods.

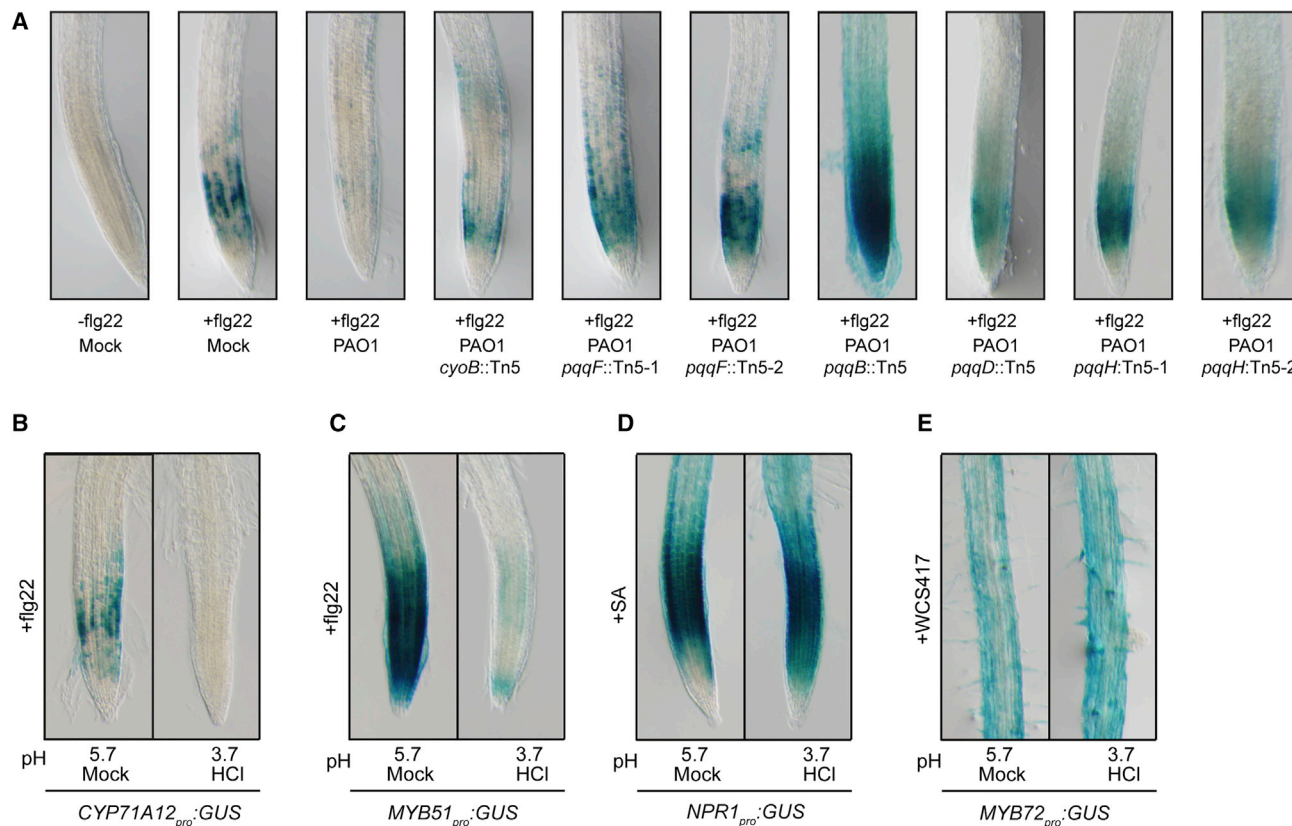


Figure 3. Mechanism to Suppress Plant Immunity Is Conserved within the Genus *Pseudomonas* and Affects Multiple Root Responses

(A) Effects of wild-type PAO1 and mutants with Tn5 insertions in *cyoB*, *pqqB*, *pqqD*, *pqqH*, and *pqqF* on flg22-induced *CYP71A12_{pro}::GUS* expression in the root elongation zone.

(B–E) Effects of pH on expression of (B) *CYP71A12_{pro}::GUS*, (C) *MYB51_{pro}::GUS*, (D) *NPR1_{pro}::GUS*, and (E) *MYB72_{pro}::GUS* in *Arabidopsis* seedlings. *CYP71A12_{pro}::GUS* and *MYB51_{pro}::GUS* were treated with 100 nM flg22. *NPR1_{pro}::GUS* was treated with 1 mM SA, and *MYB72_{pro}::GUS* was treated with WCS417. Root tips were imaged for all lines with the exception of *MYB72_{pro}::GUS*, where expression occurs in fully elongated root cells.

See also Figure S3 and STAR Methods.

To test the specificity of the effect of pH on defense gene expression, we tested 3 additional reporters for expression under acidic pH. We found that, like *CYP71A12_{pro}::GUS*, flg22-induced *MYB51_{pro}::GUS* was strongly reduced at pH 3.7 (Figures 3B and 3C). Although the binding of flg22 to its cognate receptor is affected by pH [28, 29], flg22 can still induce *CYP71A12_{pro}::GUS* in cotyledons even at pH 3.7 (Figures S2B and S2C), indicating that flg22 can be perceived by plants at low pH. Furthermore, *NPR1_{pro}::GUS* and *MYB72_{pro}::GUS*, which are induced by SA or WCS417 and WCS358, respectively [30, 31], showed no change in expression at pH 3.7 (Figures 3D and 3E). Collectively, these data indicate that MAMP-triggered defense gene expression is specifically suppressed at acidic pH, while other transcriptional activities and that of the GUS protein remain unaffected.

Mutation in *pqqF* and *cyoB* Impairs Rhizosphere Colonization by WCS358

Activation of the root immune system can affect rhizosphere microbiome assembly [17, 32–34]. Hence, we hypothesized that root immune suppression may be required for successful

colonization by rhizobacteria and expected the WCS358 derivatives *pqqF::Tn5* and *cyoB::Tn5* to have a diminished capability to colonize the *Arabidopsis* rhizosphere. We transferred *Arabidopsis* seedlings to potting soil-sand mixture, which was pre-inoculated with WCS358, *pqqF::Tn5*, or *cyoB::Tn5* with an initial population density of approximately $10^{4.5}$ colony-forming units (CFU) per gram of soil. Without a plant to support their growth, the population densities of all three strains declined over time to a similar extent (Figure 4A). In the *Arabidopsis* rhizosphere, WCS358 was able to actively colonize the roots of the *Arabidopsis* seedlings and reach population densities of approximately 10^5 CFU per gram of root in three independent experiments (Figures 4B and S4). In these three experiments, the root population densities of *pqqF::Tn5* were consistently and significantly lower than those of WCS358. Although the population densities of the *cyoB::Tn5* mutant were consistently higher than those of *pqqF::Tn5*, the *cyoB::Tn5* abundance was significantly lower than that of WCS358 in two out of three experiments. This suggests that the mutations in both *pqqF* and *cyoB* negatively affect rhizosphere colonization of WCS358.

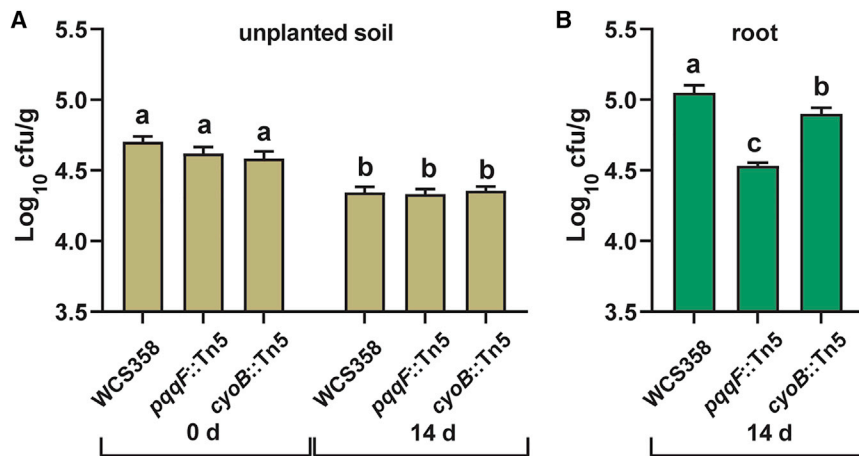


Figure 4. Mutation in *pqqF* and *cyoB* Impairs Rhizosphere Colonization by WCS358

(A) Population densities of wild-type WCS358 and its derivatives *pqqF*::Tn5 and *cyoB*::Tn5 in unplanted soil at day 0 and day 14 of Experiment I. (B) Population densities in the rhizosphere of *Arabidopsis* plants growing in that soil at day 14 of Experiment I. The y axis shows the log₁₀ of colony-forming units (CFU) per gram of bulk soil or *Arabidopsis* rhizosphere. The bars represent the mean bacterial densities of eight replicate plants. Error bars represent SEM. Letters indicate significant difference (ANOVA followed by Tukey's test; $p < 0.05$). Two replications of this experiment are shown in Figure S4. See also STAR Methods.

DISCUSSION

Since the rhizosphere is a MAMP-rich environment, the tight regulation of root immune responses is, arguably, vital to avoid constitutive activation of immune responses and associated growth-defense tradeoffs [3]. In this study, we found that the plant-beneficial rhizobacterium *P. capeferrum* WCS358 suppresses flg22-induced root immune responses by forming the organic acids GA and 2-KGA and therewith lowering the environmental pH. The observation that *P. simiae* WCS417 and *P. aeruginosa* PAO1 also similarly suppress flg22-induced root immune responses by lowering environmental pH indicates that this is a conserved mechanism among plant-associated *Pseudomonas* spp. In addition to *Pseudomonas* spp., we found that representatives of several bacterial genera, isolated from the *Arabidopsis* rhizosphere, can also suppress flg22-induced root immune responses. This indicates that the ability to quench root immune responses is shared among a taxonomically diverse group of microbes, suggesting that in a root microbiome, many community members may simultaneously contribute to host immune suppression and the prevention of growth-defense tradeoffs. While microbial traits like activation of induced systemic resistance and plant growth promotion are relatively rare in the context of the highly diverse microbial community in the rhizosphere [35, 36], environmental acidification is a broadly conserved ability of microbes [37–39]. Consequentially, if suppression of MAMP-triggered immunity is indeed an essential root microbiome function, suppression of root immunity by acidification can likely be provided by diverse members of the community. Nonetheless, we found that the mutants that failed to suppress flg22-induced root immune responses were impaired in their ability to colonize the *Arabidopsis* rhizosphere. This suggests that root immune suppression indeed enhances the colonization of the root exterior by individual microbes. Collectively, this work has identified acidification as a critical mechanism by which members of the rhizosphere microbiome can modulate host immunity to facilitate normal plant growth and development while growing in a MAMP-rich environment.

STAR★METHODS

Detailed methods are provided in the online version of this paper and include the following:

- KEY RESOURCES TABLE
- LEAD CONTACT AND MATERIALS AVAILABILITY
- EXPERIMENTAL MODEL AND SUBJECT DETAILS
 - Plant materials
 - Bacterial strains
- METHOD DETAILS
 - Bacterial culture filtrates
 - Visualization of root immune responses
 - Root immune suppression by live bacteria
 - Root immune suppression by bacterial culture filtrates
 - Tn5 mutant library generation in WCS358
 - WCS358 Tn5 mutant library screening
 - Mapping transposon insertions
 - qRT-PCR analysis
 - Detection of GA and 2-KGA
 - Effect of pH on root immune responses
 - ROS burst assays
 - Rhizosphere colonization assay
 - GUS histochemical staining assay
 - Generation of species tree
- QUANTIFICATION AND STATISTICAL ANALYSIS
- DATA AND CODE AVAILABILITY

SUPPLEMENTAL INFORMATION

Supplemental Information can be found online at <https://doi.org/10.1016/j.cub.2019.09.015>.

ACKNOWLEDGMENTS

We thank Dr. Frederick M. Ausubel (Massachusetts General Hospital, Boston, MA) for kindly providing the *Arabidopsis* GUS reporter lines used in this study, Dr. Víctor de Lorenzo (Centro Nacional de Biotecnología, Madrid, Spain) for kindly providing *Escherichia coli* donor and helper strains used for triparental mating, and Dr. Dananjeyan Balachandrar (Tamil Nadu Agricultural University, Coimbatore, Tamil Nadu, India) for assistance in the lab. This work was supported by European Research Council Advanced Grant 269072 (to

C.M.J.P.), an NSERC Discovery Grant (NSERC-RGPIN-2016-04121) (to C.H.H.), and China Scholarship Council fellowships (to K.Y. and Y.L.).

AUTHOR CONTRIBUTIONS

K.Y., C.H.H., P.A.H.M.B., C.M.J.P., and R.L.B. designed research and wrote the paper; K.Y., Y.L., R.T., N.S., S.J.L.v.K., I.A.S., A.J.H.v.D., E.L., and R.L.B. performed research; K.Y., Y.L., I.A.S., C.H.H., P.A.H.M.B., C.M.J.P., and R.L.B. analyzed data.

DECLARATION OF INTERESTS

The authors declare no competing interests.

Received: May 23, 2019

Revised: August 2, 2019

Accepted: September 6, 2019

Published: October 24, 2019

REFERENCES

- Berendsen, R.L., Pieterse, C.M.J., and Bakker, P.A.H.M. (2012). The rhizosphere microbiome and plant health. *Trends Plant Sci.* *17*, 478–486.
- Zamioudis, C., and Pieterse, C.M.J. (2012). Modulation of host immunity by beneficial microbes. *Mol. Plant Microbe Interact.* *25*, 139–150.
- Pel, M.J., and Pieterse, C.M.J. (2013). Microbial recognition and evasion of host immunity. *J. Exp. Bot.* *64*, 1237–1248.
- Huot, B., Yao, J., Montgomery, B.L., and He, S.Y. (2014). Growth-defense tradeoffs in plants: a balancing act to optimize fitness. *Mol. Plant* *7*, 1267–1287.
- Meziane, H., VAN DER Sluis, I., VAN Loon, L.C., Höfte, M., and Bakker, P.A.H.M. (2005). Determinants of *Pseudomonas putida* WCS358 involved in inducing systemic resistance in plants. *Mol. Plant Pathol.* *6*, 177–185.
- Berendsen, R.L., van Verk, M.C., Stringlis, I.A., Zamioudis, C., Tommassen, J., Pieterse, C.M.J., and Bakker, P.A.H.M. (2015). Unearthing the genomes of plant-beneficial *Pseudomonas* model strains WCS358, WCS374 and WCS417. *BMC Genomics* *16*, 539.
- Pieterse, C.M., van Wees, S.C., Hoffland, E., van Pelt, J.A., and van Loon, L.C. (1996). Systemic resistance in *Arabidopsis* induced by biocontrol bacteria is independent of salicylic acid accumulation and pathogenesis-related gene expression. *Plant Cell* *8*, 1225–1237.
- Millet, Y.A., Danna, C.H., Clay, N.K., Songnuan, W., Simon, M.D., Werck-Reichhart, D., and Ausubel, F.M. (2010). Innate immune responses activated in *Arabidopsis* roots by microbe-associated molecular patterns. *Plant Cell* *22*, 973–990.
- Boller, T., and Felix, G. (2009). A renaissance of elicitors: perception of microbe-associated molecular patterns and danger signals by pattern-recognition receptors. *Annu. Rev. Plant Biol.* *60*, 379–406.
- Xin, X.-F., Nomura, K., Aung, K., Velásquez, A.C., Yao, J., Boutrot, F., Chang, J.H., Zipfel, C., and He, S.Y. (2016). Bacteria establish an aqueous living space in plants crucial for virulence. *Nature* *539*, 524–529.
- Denoux, C., Galletti, R., Mammarella, N., Gopalan, S., Werck, D., De Lorenzo, G., Ferrari, S., Ausubel, F.M., and Dewdney, J. (2008). Activation of defense response pathways by OGs and Flg22 elicitors in *Arabidopsis* seedlings. *Mol. Plant* *1*, 423–445.
- Hacquard, S., Spaepen, S., Garrido-Oter, R., and Schulze-Lefert, P. (2017). Interplay between innate immunity and the plant microbiota. *Annu. Rev. Phytopathol.* *55*, 565–589.
- Lopez-Gomez, M., Sandal, N., Stougaard, J., and Boller, T. (2012). Interplay of flg22-induced defence responses and nodulation in *Lotus japonicus*. *J. Exp. Bot.* *63*, 393–401.
- Trdá, L., Fernandez, O., Boutrot, F., Héloir, M.C., Kelloniemi, J., Daire, X., Adrian, M., Clément, C., Zipfel, C., Dorey, S., and Poinssot, B. (2014). The grapevine flagellin receptor VvFLS2 differentially recognizes flagellin-derived epitopes from the endophytic growth-promoting bacterium *Burkholderia phytofirmans* and plant pathogenic bacteria. *New Phytol.* *201*, 1371–1384.
- Stringlis, I.A., Proietti, S., Hickman, R., Van Verk, M.C., Zamioudis, C., and Pieterse, C.M.J. (2018). Root transcriptional dynamics induced by beneficial rhizobacteria and microbial immune elicitors reveal signatures of adaptation to mutualists. *Plant J.* *93*, 166–180.
- Zipfel, C., and Oldroyd, G.E. (2017). Plant signalling in symbiosis and immunity. *Nature* *543*, 328–336.
- Berendsen, R.L., Vismans, G., Yu, K., Song, Y., de Jonge, R., Burgman, W.P., Burmölle, M., Herschend, J., Bakker, P.A.H.M., and Pieterse, C.M.J. (2018). Disease-induced assemblage of a plant-beneficial bacterial consortium. *ISME J.* *12*, 1496–1507.
- Wei, Q., Ran, T., Ma, C., He, J., Xu, D., and Wang, W. (2016). Crystal structure and function of PqqF protein in the pyrroloquinoline quinone biosynthetic pathway. *J. Biol. Chem.* *291*, 15575–15587.
- Shen, Y.Q., Bonnot, F., Imsand, E.M., RoseFigura, J.M., Sjölander, K., and Klinman, J.P. (2012). Distribution and properties of the genes encoding the biosynthesis of the bacterial cofactor, pyrroloquinoline quinone. *Biochemistry* *51*, 2265–2275.
- Stenberg, F., von Heijne, G., and Daley, D.O. (2007). Assembly of the cytochrome bo3 complex. *J. Mol. Biol.* *371*, 765–773.
- Morales, G., Ugidos, A., and Rojo, F. (2006). Inactivation of the *Pseudomonas putida* cytochrome o ubiquinol oxidase leads to a significant change in the transcriptome and to increased expression of the CIO and cbb3-1 terminal oxidases. *Environ. Microbiol.* *8*, 1764–1774.
- Fender, J.E., Bender, C.M., Stella, N.A., Lahr, R.M., Kalivoda, E.J., and Shanks, R.M. (2012). *Serratia marcescens* quinoprotein glucose dehydrogenase activity mediates medium acidification and inhibition of prodigiosin production by glucose. *Appl. Environ. Microbiol.* *78*, 6225–6235.
- Lee, H., Khatri, A., Plotnikov, J.M., Zhang, X.C., and Sheen, J. (2012). Complexity in differential peptide-receptor signaling: response to Segonzac et al. and Mueller et al. commentaries. *Plant Cell* *24*, 3177–3185.
- Cessna, S.G., Sears, V.E., Dickman, M.B., and Low, P.S. (2000). Oxalic acid, a pathogenicity factor for *Sclerotinia sclerotiorum*, suppresses the oxidative burst of the host plant. *Plant Cell* *12*, 2191–2200.
- Jacobs, M.A., Alwood, A., Thaipisuttikul, I., Spencer, D., Haugen, E., Ernst, S., Will, O., Kaul, R., Raymond, C., Levy, R., et al. (2003). Comprehensive transposon mutant library of *Pseudomonas aeruginosa*. *Proc. Natl. Acad. Sci. USA* *100*, 14339–14344.
- De Meyer, G., and Höfte, M. (1997). Salicylic acid produced by the rhizobacterium *Pseudomonas aeruginosa* TNSK2 induces resistance to leaf infection by *Botrytis cinerea* on bean. *Phytopathology* *87*, 588–593.
- Rahme, L.G., Stevens, E.J., Wolfort, S.F., Shao, J., Tompkins, R.G., and Ausubel, F.M. (1995). Common virulence factors for bacterial pathogenicity in plants and animals. *Science* *268*, 1899–1902.
- Bauer, Z., Gómez-Gómez, L., Boller, T., and Felix, G. (2001). Sensitivity of different ecotypes and mutants of *Arabidopsis thaliana* toward the bacterial elicitor flagellin correlates with the presence of receptor-binding sites. *J. Biol. Chem.* *276*, 45669–45676.
- Meindl, T., Boller, T., and Felix, G. (2000). The bacterial elicitor flagellin activates its receptor in tomato cells according to the address-message concept. *Plant Cell* *12*, 1783–1794.
- Cao, H., Glazebrook, J., Clarke, J.D., Volko, S., and Dong, X. (1997). The *Arabidopsis* NPR1 gene that controls systemic acquired resistance encodes a novel protein containing ankyrin repeats. *Cell* *88*, 57–63.
- Zamioudis, C., Korteland, J., Van Pelt, J.A., van Hamersveld, M., Dombrowski, N., Bai, Y., Hanson, J., Van Verk, M.C., Ling, H.-Q., Schulze-Lefert, P., and Pieterse, C.M. (2015). Rhizobacterial volatiles and photosynthesis-related signals coordinate MYB72 expression in *Arabidopsis* roots during onset of induced systemic resistance and iron-deficiency responses. *Plant J.* *84*, 309–322.
- Lebeis, S.L., Paredes, S.H., Lundberg, D.S., Breakfield, N., Gehring, J., McDonald, M., Malfatti, S., Glavina del Rio, T., Jones, C.D., Tringe, S.G., and Dangl, J.L. (2015). PLANT MICROBIOME. Salicylic acid modulates

- colonization of the root microbiome by specific bacterial taxa. *Science* 349, 860–864.
33. Liu, H., Carvalhais, L.C., Schenk, P.M., and Dennis, P.G. (2017). Effects of jasmonic acid signalling on the wheat microbiome differ between body sites. *Sci. Rep.* 7, 41766.
 34. Carvalhais, L.C., Dennis, P.G., Badri, D.V., Kidd, B.N., Vivanco, J.M., and Schenk, P.M. (2015). Linking jasmonic acid signaling, root exudates, and rhizosphere microbiomes. *Mol. Plant Microbe Interact.* 28, 1049–1058.
 35. Pieterse, C.M.J., Zamioudis, C., Berendsen, R.L., Weller, D.M., Van Wees, S.C.M., and Bakker, P.A.H.M. (2014). Induced systemic resistance by beneficial microbes. *Annu. Rev. Phytopathol.* 52, 347–375.
 36. Vannier, N., Agler, M., and Hacquard, S. (2019). Microbiota-mediated disease resistance in plants. *PLoS Pathog.* 15, e1007740.
 37. Dutton, M.V., and Evans, C.S. (1996). Oxalate production by fungi: its role in pathogenicity and ecology in the soil environment. *Can. J. Microbiol.* 42, 881–895.
 38. Jones, D.L. (1998). Organic acids in the rhizosphere – a critical review. *Plant Soil* 205, 25–44.
 39. Rodríguez, H., Fraga, R., Gonzalez, T., and Bashan, Y. (2006). Genetics of phosphate solubilization and its potential applications for improving plant growth-promoting bacteria. *Plant Soil* 287, 15–21.
 40. Yu, D., Chen, C., and Chen, Z. (2001). Evidence for an important role of WRKY DNA binding proteins in the regulation of NPR1 gene expression. *Plant Cell* 13, 1527–1540.
 41. Melnyk, R.A., Hossain, S.S., and Haney, C.H. (2019). Convergent gain and loss of genomic islands drive lifestyle changes in plant-associated *Pseudomonas*. *ISME J.* 13, 1575–1588.
 42. Gómez-Gómez, L., and Boller, T. (2000). FLS2: an LRR receptor-like kinase involved in the perception of the bacterial elicitor flagellin in *Arabidopsis*. *Mol. Cell* 5, 1003–1011.
 43. Van Wees, S.C.M., Van Pelt, J.A., Bakker, P.A.H.M., and Pieterse, C.M.J. (2013). Bioassays for assessing jasmonate-dependent defenses triggered by pathogens, herbivorous insects, or beneficial rhizobacteria. In *Jasmonate Signaling: Methods in Molecular Biology (Methods and Protocols)*, A. Goossens, and L. Pauwels, eds. (Humana Press), pp. 35–49.
 44. Murashige, T., and Skoog, F. (1962). A revised medium for rapid growth and bioassays with tobacco tissue cultures. *Physiol. Plant.* 15, 473–497.
 45. Navarro, L., Bari, R., Achard, P., Lisón, P., Nemri, A., Harberd, N.P., and Jones, J.D. (2008). DELLAs control plant immune responses by modulating the balance of jasmonic acid and salicylic acid signaling. *Curr. Biol.* 18, 650–655.
 46. Martínez-García, E., Calles, B., Arévalo-Rodríguez, M., and de Lorenzo, V. (2011). pBAM1: an all-synthetic genetic tool for analysis and construction of complex bacterial phenotypes. *BMC Microbiol.* 11, 38.
 47. King, E.O., Ward, M.K., and Raney, D.E. (1954). Two simple media for the demonstration of pyocyanin and fluorescein. *J. Lab. Clin. Med.* 44, 301–307.
 48. Hickman, R., Van Verk, M.C., Van Dijken, A.J.H., Mendes, M.P., Vroegop-Vos, I.A., Caarls, L., Steenberg, M., Van der Nagel, I., Wesselink, G.J., Jironkin, A., et al. (2017). Architecture and dynamics of the jasmonic acid gene regulatory network. *Plant Cell* 29, 2086–2105.
 49. Czechowski, T., Bari, R.P., Stitt, M., Scheible, W.-R., and Udvardi, M.K. (2004). Real-time RT-PCR profiling of over 1400 *Arabidopsis* transcription factors: unprecedented sensitivity reveals novel root- and shoot-specific genes. *Plant J.* 38, 366–379.
 50. Schmittgen, T.D., and Livak, K.J. (2008). Analyzing real-time PCR data by the comparative C(T) method. *Nat. Protoc.* 3, 1101–1108.
 51. Mammarella, N.D., Cheng, Z., Fu, Z.Q., Daudi, A., Bolwell, G.P., Dong, X., and Ausubel, F.M. (2015). Apoplastic peroxidases are required for salicylic acid-mediated defense against *Pseudomonas syringae*. *Phytochemistry* 112, 110–121.

STAR★METHODS

KEY RESOURCES TABLE

REAGENT or RESOURCE	SOURCE	IDENTIFIER
Bacterial Strains		
<i>Pseudomonas simiae</i> WCS417	[15]	N/A
<i>Pseudomonas capeferrum</i> WCS358	[15]	N/A
<i>Escherichia coli</i> CC118λpir + pBAM1	[7]	N/A
<i>E. coli</i> HB101 + pRK600	[7]	N/A
<i>Pseudomonas aeruginosa</i> PAO1	[34]	N/A
<i>Pseudomonas aeruginosa</i> PAO1 PW4440 (pqqF-H07::ISphoA/hah)	[34]	N/A
<i>Pseudomonas aeruginosa</i> PAO1 PW4439 (pqqF-A09::ISlacZ/hah)	[34]	N/A
<i>Pseudomonas aeruginosa</i> PAO1 PW3391 (cyoB-G03::ISlacZ/hah)	[34]	N/A
<i>Pseudomonas aeruginosa</i> PAO1 PW4455 (pqqB-B05::ISlacZ/hah)	[34]	N/A
<i>Pseudomonas aeruginosa</i> PAO1 PW4456 (pqqD-E02::ISlacZ/hah)	[34]	N/A
<i>Pseudomonas aeruginosa</i> PAO1 PW4459 (pqqH-G01::ISlacZ/hah)	[34]	N/A
<i>Pseudomonas aeruginosa</i> PAO1 PW4460 (pqqH-G11::ISphoA/hah)	[34]	N/A
Chemicals, Peptides, and Recombinant Proteins		
Fig22 ^{Pa}	GenScript	Cat# RP19986
Fig22 ⁴¹⁷ : QRLSTGLSINSAKDNASGLQIS	GenScript	N/A
Fig22 ³⁵⁸ : QRLSSGLRINSAKDDAAGLQIA	GenScript	N/A
Rifampicin, CAS# 13292-46-1	Duchefa	Cat# R0146
Kanamycin, CAS# 25389-94-0	Duchefa	Cat# K0126
Nalidixic acid, CAS# 389-08-2	Duchefa	Cat# N0136
Ampicillin, CAS# 69-52-3	Duchefa	Cat# A0104
Chloramphenicol, CAS# 56-75-7	Duchefa	Cat# C0113
Delvolid	DSM	Cat# 11c30kf01
D-Gluconic acid, CAS# 526-95-4	Sigma-Aldrich	Cat# G1951
D-Gluconic acid sodium salt, CAS# 527-07-1	Sigma-Aldrich	Cat# G9005
2-Keto-D-gluconic acid hemi-calcium salt hydrate, CAS# 140352-40-6	Sigma-Aldrich	Cat# K6250
Luminol derivative L-012, CAS# 521-31-3	Sigma-Aldrich	Cat# A8511
Horseradish peroxidase	Sigma-Aldrich	Cat# 516531
Critical Commercial Assays		
GenElute Bacterial Genomic DNA Kits	Sigma-Aldrich	Cat# NA2110
Experimental Models: Organisms/Strains		
<i>Arabidopsis thaliana</i> CYP71A12 _{pro} -GUS	[16]	N/A
<i>Arabidopsis thaliana</i> MYB51 _{pro} -GUS	[16]	N/A
<i>Arabidopsis thaliana</i> WRKY11 _{pro} -GUS	[16]	N/A
<i>Arabidopsis thaliana</i> NPR1 _{pro} -GUS	[40]	N/A
<i>Arabidopsis thaliana</i> MYB72 _{pro} -GUS	[41]	N/A
Oligonucleotides		
Primer: PP2AA3_Fw At1g13320 5'-TAACGTGGCCAAAATGATGC-3'	[14]	N/A
PP2AA3_Rev At1g13320 5'-GTTCTCCACAACCGCTTGGT-3'	[14]	N/A
CYP71A12_Fw At2g30750 5'-GATTATCACCTCGGTTCT-3'	[14]	N/A
CYP71A12_Rev At2g30750 5'-CCACTAATACTCCCAGATTA-3'	[14]	N/A
Software and Algorithms		
CLC Main Workbench 6.0	QIAGEN	https://www.qiagenbioinformatics.com
GraphPad Prism 7	GraphPad Software	https://www.graphpad.com/

LEAD CONTACT AND MATERIALS AVAILABILITY

Further information and requests for resources and reagents should be directed to and will be fulfilled by the Lead Contact, Roeland Berendsen (r.l.berendsen@uu.nl). This study did not generate new reagents.

EXPERIMENTAL MODEL AND SUBJECT DETAILS

Plant materials

In this study, we used the *Arabidopsis thaliana* wild-type accessions Col-0 and Ws-0, and Col-0 mutant *fls2* [42]. Additionally, we used GUS reporter lines *CYP71A12_{pro}:GUS*, *MYB51_{pro}:GUS* and *WRKY11_{pro}:GUS*, *NPR1_{pro}:GUS* and *MYB72_{pro}:GUS* in Col-0 background, and *CYP71A12_{pro}:GUS* in the background of Col-0 mutants *sid2-2*, *npr1-1*, *jar1-1* and *jln1-7* [8, 40]. With the exception of the *MYB72_{pro}:GUS* reporter, all *Arabidopsis* GUS reporter lines were kindly provided by Dr. Frederick M. Ausubel (Harvard Medical School, Boston, MA). For experiments performed *in vitro*, *Arabidopsis* seeds were surface sterilized for 4 h with chlorine gas in a bell jar containing a beaker filled with 100 mL bleach and 3.2 mL 37% HCl. Surface-sterilized seeds were left in the flow cabinet for an additional 2 h to clear the chlorine gas. For all experiments, *Arabidopsis* seeds were incubated at 4°C for a 2-day stratification before being moved to the plant growth chambers [43].

Bacterial strains

Pseudomonas simiae WCS417 and *Pseudomonas capeferrum* WCS358 were inoculated in liquid KB supplemented with 150 µg ml⁻¹ of rifampicin and incubated at 28°C for 16 h. Bacterial strains from a collection of rhizobacteria isolated from *Arabidopsis* roots [17] were inoculated in 1/10 strength liquid tryptic soy broth and incubated at 20°C for 48 h. Bacterial strains from the mutant library were inoculated on agar-solidified KB plates supplemented with 150 µg ml⁻¹ of rifampicin, 50 µg ml⁻¹ of kanamycin and 100 µg ml⁻¹ of nalidixic acid and incubated at 28°C for 24 h. Before usage, fresh bacterial cultures were pelleted by centrifuging at 5000 rpm for 5 min, gently washed and resuspended in 10 mM MgSO₄. This pellet-wash-resuspend step was repeated three times after which the bacterial suspension was adjusted to the desired density based on optical density at 660 nm (OD₆₆₀).

METHOD DETAILS

Bacterial culture filtrates

Col-0 seedlings were sown in 12-well microtiter plates (10 to 12 seeds per well) with each well containing 1 mL Murashige and Skoog medium [44] supplemented with 0.5 g l⁻¹ of MES monohydrate and 5 g l⁻¹ of sucrose with the initial pH adjusted to 5.7 (MS medium). Plants were grown in a plant growth chamber under long-day conditions (21°C, 16 h light/8 h dark, light intensity 100 µmol m⁻² s⁻¹) [8] for ten days, after which root exudates were collected by filtering the medium through 0.2 µm Millipore filters (Merck KGaA, Darmstadt, Germany). For the preparation of bacterial culture filtrates, 1 mL of these root exudates were subsequently inoculated with bacterial suspensions, prepared as described above, to an initial density of OD₆₆₀ = 0.002, and placed in each well of a 12-well microtiter plate in a plant growth chamber simulating long-day conditions [8]. After 22 h, bacterial cultures were filtered through 0.2 µm Millipore filters and stored at -20°C. The heated-culture filtrates were prepared by heating the culture filtrates for 1 h at 100°C.

Visualization of root immune responses

All flg22 peptides (GenScript, Piscataway, NJ) were prepared in Milli-Q water (Millipore Corp., Bedford, MA) as 100 µM stock solutions. To visually assess GUS activity in the roots, seeds of *Arabidopsis* transgenic lines were sown in 12-well microtiter plates. Each well contained 10 to 12 seeds and was filled with 1 mL MS medium. The pH of MS medium was adjusted to 5.7 with KOH. Seeds were allowed to germinate and grow in a plant growth chamber simulating long-day conditions. 100 nM flg22 was added to the growth medium of 10-day-old *Arabidopsis* seedlings in 12-well microtiter plates. GUS histochemical staining assays were performed at 3 h (for *MYB51_{pro}:GUS* and *WRKY11_{pro}:GUS*) or 5 h (for *CYP71A12_{pro}:GUS*) after flg22 treatment [8].

The assay to determine the growth-inhibiting effect of flg22 was performed as described previously with modifications [45]. Briefly, seeds of Col-0, *fls2* or Ws-0 were sown in 12-well microtiter plates. Each well contained 2 seeds and was filled with 1 mL MS medium. After 5 days, 100 nM flg22 epitopes derived from *P. aeruginosa* PAO1, *P. simiae* WCS417 or *P. capeferrum* WCS358 (flg22^{Pa}, flg22⁴¹⁷, or flg22³⁵⁸) were added to the growth medium of 5-day-old *Arabidopsis* seedlings and the weight of the seedlings was weighed at 7 days after flg22 treatment. In most experiments we routinely used flg22^{Pa} and referred to as flg22 unless specifically specified otherwise.

Root immune suppression by live bacteria

To assess the immune suppression ability of live bacteria, rhizobacterial strains were pre-inoculated to the growth medium of 9-day-old *Arabidopsis* seedlings in 12-well microtiter plates to a final density of OD₆₆₀ = 0.002 and 100 nM flg22 was added to the growth medium after 18 h. GUS histochemical staining assays were performed at 3 h (for *MYB51_{pro}:GUS* and *WRKY11_{pro}:GUS*) or 5 h (for *CYP71A12_{pro}:GUS*) after flg22 treatment [8].

Root immune suppression by bacterial culture filtrates

To assess the immune suppression ability of bacterial culture filtrates, culture filtrates or heat-treated culture filtrates were used to replace the growth medium of 10-day-old *Arabidopsis* seedlings in 12-well microtiter plates and 100 nM flg22 was added to bacterial culture filtrates after 1.5 h. GUS histochemical staining assays were performed at 5 h after flg22 treatment [8].

Tn5 mutant library generation in WCS358

A mini-Tn5 transposon insertion mutant library for *P. capeferrum* WCS358 was generated through triparental mating using donor strain *Escherichia coli* CC118 λ pir harboring pBAM1 and helper strain *E. coli* HB101 harboring pRK600, kindly provided by Dr. Víctor de Lorenzo (Centro Nacional de Biotecnología, Madrid, Spain). Tri parental mating was accomplished as described by Martínez-García et al. [46], wherewith it should be noted that the recipient strain WCS358 was inoculated in liquid King's medium B [47] supplemented with 150 $\mu\text{g ml}^{-1}$ of rifampicin. Moreover, individual mutant colonies of the recipient strain WCS358 were selected on agar-solidified LB medium supplemented with 150 $\mu\text{g ml}^{-1}$ of rifampicin, 50 $\mu\text{g ml}^{-1}$ of kanamycin and 100 $\mu\text{g ml}^{-1}$ of nalidixic acid at 28°C.

WCS358 Tn5 mutant library screening

To screen the bacterial mutant library, seeds of *Arabidopsis* transgenic line *CYP71A12_{pro}:GUS* were sown in 96-well microtiter plates. Each well contained 1 seed and was filled with 200 μL MS medium. Seeds were allowed to germinate and grow in a plant growth chamber simulating long-day conditions. Live bacteria were pre-inoculated to the growth medium of 9-day-old *Arabidopsis* seedlings to a final density of $\text{OD}_{660} = 0.002$ and 100 nM flg22 was added to the growth medium after 18 h. GUS histochemical staining assays were performed at 5 h after flg22 treatment.

To assess the growth of selected mutants in root exudates, bacterial suspension was inoculated in 96-well microtiter plates containing 200 μL root exudates per well, at an initial bacterial density at $\text{OD}_{660} = 0.002$. Bacterial densities were assessed at 0 and 24 h after inoculation, by plating serial dilutions on agar-solidified KB plates supplemented with antibiotics as described above. The plates were incubated at 28°C for 24 h and numbers of colony-forming units (CFU) were determined.

Mapping transposon insertions

Genomic DNA of the mutants was isolated from bacterial cultures using GenElute Bacterial Genomic DNA Kits (Sigma-Aldrich, St. Louis, MO). Arbitrary PCR was used to determine the localization of transposon insertions using primers described previously [46]. The product from the second PCR round was purified with Agencourt AMPure XP beads (Beckman Coulter, Indianapolis, IN) and sequenced using ME-O-intF primer (Macrogen, Seoul, South Korea). Sequencing results were analyzed in CLC Main Workbench (QIAGEN, Venlo, the Netherlands).

qRT-PCR analysis

Total RNA extraction for qRT-PCR gene expression analysis was performed as described previously on 18-days-old seedlings [48]. Transcript levels were calculated relative to the reference gene *At1g13320* [49] using the $2^{-\Delta\text{CT}}$ method [50].

Detection of GA and 2-KGA

GA and 2-KGA concentrations in bacterial culture filtrates were determined using ultra-performance liquid chromatography-mass spectrometry (UPLC-MS). Compounds were separated on a Waters Acquity UPLC BEH Amide Column (130Å, 1.7 μm particle size, 2.1 mm X 50 mm) by an Acquity UPLC system (Waters, Milford, MA, USA). The mobile phase A was 90% water, 10% acetonitrile, 0.1% formic acid and the mobile phase B was 100% acetonitrile, 0.1% formic acid. All solutions were ULC/MS grade from Biosolve BV (Valkenswaard, the Netherlands) The gradient was set from 10% to 90% with a flow rate of 0.25 mL min^{-1} . The run time was 6 min and the inject volume was 1 μL . Mass spectrometric detection was performed in negative ionization mode m/z 50 – 1250 and SIR of 2 channels m/z 193 and m/z 195 on a Waters Acquity QDa detector (Waters, Milford, MA, USA). GA and 2-KGA was quantified by peak area obtained from standards for D-Gluconic acid sodium salt (Sigma-Aldrich, St. Louis, MO) and 2-Keto-D-gluconic acid hemi-calcium salt hydrate (Sigma-Aldrich, St. Louis, MO).

Effect of pH on root immune responses

The pH-adjusted root exudates or MS medium were prepared using 10% HCl or 10% D-gluconic acid to adjust the pH of root exudates or MS medium to 3.7 or other desired pH. To assess the effect of pH on flg22-induced *CYP71A12_{pro}:GUS* expression, pH-adjusted root exudates or MS medium, both were used to replace the growth medium of 9-day-old *Arabidopsis* seedlings in 12-well microtiter plates and 100 nM flg22 was added to pH-adjusted root exudates after 18 h. Alternatively, pH-adjusted root exudates or MS medium were used to replace the growth medium of 10-day-old *Arabidopsis* seedlings and 100 nM flg22 was added to pH-adjusted root exudates at the same time. GUS histochemical staining assays were performed at 5 h after flg22 treatment.

ROS burst assays

Reactive oxygen burst assays were performed on a Tecan Plate reader using the luminol reagent as described with modifications [51]. Seedlings were germinated in white, flat-bottom, 96 well plates with 200 μL of sterile MS (with 0.5% sucrose) media (one seed/well). Plants were grown under long-day conditions (23°C, 16 h light/8 h dark). On day 9, media in each well was replaced

with 200 μL of sterile water. Ox-Burst reagent was prepared the next day by adding Luminol derivative L-012 (final concentration of 100 μM), Horseradish Peroxidase (final concentration of 20 $\mu\text{g}/\text{mL}$) and flg22 (final concentration of 1 μM) to 24 mL of water, or previously adjusted to a pH of 3.7 by 10% D-gluconic acid or 10% HCl. ROS reagents were added immediately before reading. Chemiluminescence was measured using a Tecan plate reader for 60 cycles with kinetic interval of 1 min and integration time of 350 ms. Experiments were performed at least 2 independent times.

Rhizosphere colonization assay

To assess bacterial rhizosphere colonization, *Arabidopsis* Col-0 seeds were sown on river sand saturated with modified half-strength Hoagland solution [43]. The seeds were allowed to germinate and grow in a plant growth chamber simulating short-day conditions for 12 days. Bacterial suspensions were mixed into a potting soil-sand mixture at an initial bacterial density of approximately 4.5×10^4 CFU g^{-1} soil as described previously [7]. *Arabidopsis* seedlings were then transferred to 60 mL pots containing soil pre-inoculated with bacteria. Unplanted bulk soil samples and rhizosphere plus root samples were harvested at 0 and 14 days after transplanting. All samples were placed in 2 mL pre-weighed Eppendorf tubes containing 3 glass beads, weighed and suspended in 1 mL 10 mM MgSO_4 using TissueLyser II (QIAGEN, Venlo, the Netherlands) with a frequency of 30 beats per second. Bacterial densities were assessed by plating serial dilutions of the samples on agar-solidified KB medium supplemented with 150 $\mu\text{g ml}^{-1}$ rifampicin, 50 $\mu\text{g ml}^{-1}$ ampicillin, 13 $\mu\text{g ml}^{-1}$ chloramphenicol and 100 $\mu\text{g ml}^{-1}$ Delvocid (DSM, Heerlen, the Netherlands). The plates were incubated at 28°C for 24 h and then numbers of CFU were determined.

GUS histochemical staining assay

The growth medium of *Arabidopsis* seedlings was replaced with an equal amount of freshly-prepared GUS substrate solution (50 mM sodium phosphate with a pH at 7, 10 mM EDTA, 0.5 mM $\text{K}_4[\text{Fe}(\text{CN})_6]$, 0.5 mM $\text{K}_3[\text{Fe}(\text{CN})_6]$, 0.5 mM X-Gluc, and 0.01% Silwet L-77) [8]. Plates were incubated in the dark at room temperature for 16 h. The GUS substrate solution was subsequently replaced with 96% ethanol and ethanol was refreshed after 24 h. *Arabidopsis* seedlings were then cleared in a solution of chloral hydrate: glycerol: water (8: 1: 2, v/v/v) [31] and pictures were taken using an Axioskop 2 stereo microscope (Zeiss, Jena, Germany) with a Lumenera Infinity 1 camera (Lumenera Corporation, Ottawa, ON) and the software Image-Pro Insight 9.1 (Media Cybernetics, Rockville, MD).

Generation of species tree

The species tree used in Figure S3 was generated as described using 122 single-copy genes we previously found to be conserved in all bacteria [41]. Presence/absence determination of the *pqqABCDEH* genes, *pqqF* and *cyoABCDE* was determined using the PyParanoid comparative genomics tool [41]. The database includes over 3800 genomes of *Pseudomonas* spp. We used the annotated sequences for *pqqABCDEH* genes, *pqqF* and *cyoABCDE* from *P. aeruginosa* PAO1 to query the database and then plotted the presence/absence data against the species tree.

QUANTIFICATION AND STATISTICAL ANALYSIS

The analyses of variance in Figures 1E, 2B, 2E, 4A, 4B, S4A, and S4B, and the Student's t test in Figure 2D were performed using GraphPad Prism 7 (GraphPad Software, La Jolla, CA). The statistical details of these experiments (e.g., the number of replicates, the definition of center, and the dispersion and precisions measures) are given in the respective figure legends.

DATA AND CODE AVAILABILITY

The published article includes all data generated or analyzed during this study.